Adsorption and dissociation of O_2 at Be(0001): First-principles prediction of an energy barrier on the adiabatic potential energy surface

Ping Zhang,[1,2] Bo Sun,[1] and Yu Yang[1,3]

[1]*LCP, Institute of Applied Physics and Computational Mathematics, P.O. Box 8009, Beijing 100088, People's Republic of China*

[2]*Center for Applied Physics and Technology, Peking University, Beijing 100871, People's Republic of China*

[3]*Department of Physics and Center for Advanced Study, Tsinghua University, Beijing 100084, People's Republic of China*

(Received 8 December 2008; revised manuscript received 13 February 2009; published 13 April 2009)

The adsorption and dissociation of O_2 molecules at the Be(0001) surface is studied by using density-functional theory within the generalized gradient approximation and a supercell approach. The physisorbed and chemisorbed molecular precursor states are identified to be along the parallel and vertical channels, respectively. It is shown that the vertical channel with O_2 being at the hcp hollow sites of the Be(0001) surface is the most stable channel for the molecular chemisorption. The electronic and magnetic properties of this most stable chemisorbed molecular state are studied, which show that the electrons transfer forth and back between the spin-resolved antibonding π^* molecular orbitals and surface Be *sp* states. A distinct covalent weight in the molecule-metal bond is also shown. The dissociation of O_2 is determined by calculating the adiabatic potential energy surfaces, wherein the T-*Y* channel is found to be the most stable and favorable for dissociative adsorption of O_2. Remarkably, we predict that unlike other simple *sp* metal surfaces such as Al(111) and Mg(0001), the *adiabatic* dissociation process of O_2 at Be(0001) is an activated type with a sizeable energy barrier.

DOI: 10.1103/PhysRevB.79.165416 PACS number(s): 68.43.Bc, 82.20.Kh, 82.45.Jn, 34.80.Ht

I. INTRODUCTION

It is of great scientific importance to understand the behaviors of diatomic molecules at solid surfaces, including their adsorption and dissociation, and corresponding energy barriers during the bond breaking and bond formation at the surfaces.[1,2] Of all prototypes, the interaction of O_2 molecules with metal surfaces has gained a lot of interest for many technologically relevant processes such as heterogeneous catalysis and corrosion.[3] Theoretically, *ab initio* modeling has been successfully used over a wide range to study the adsorption and dissociation of O_2 molecules at transition-metal surfaces. By calculating the adiabatic potential energy surface (PES), it has been found that O_2 molecules will spontaneously dissociate while adsorbing at reactive transition-metal surfaces such as iron.[4] For noble transition metals such as gold,[5] silver,[6,7] platinum,[5,8,9] and nickel,[9] the adsorption of O_2 turns out to depend on the ambient temperature. Remarkably, in all the abovementioned transition-metal systems, the concept of adiabatic PES works very well in explaining and predicting a large amount of physical/chemical phenomena during dissociation process of O_2.

When the attention is focused on the simple *sp* metals such as Al(111), however, an uncomfortable gap opens between *ab initio* prediction and experimental observations. The most notable is the long-term enigma of low initial sticking probability of thermal O_2 molecules at Al(111), which has been measured by many independent experiments[10,11] but cannot be reproduced by adiabatic state-of-the-art density-functional theory (DFT) calculations.[12–14] The central problem is that the adiabatic DFT calculations were unable to find any sizeable barriers on the adiabatic PES, whose presence, however, is essential for the explanation of the experimental finding. This has led to speculations that nonadiabatic effects may play an important role in the oxygen dissociation process at the Al(111) surface.[13,15–20] Recently, a semiquantitative agreement with the experimental data is achieved by nonadiabatically confining the trajectories of the approaching O_2 molecules to the spin-triplet PES.[21] Until now, however, it still remains unclear how and in what chemical circumstance this spin-selection rule is reasonable, and different opinions exist in the literature.[22] For oxygen dissociation at another simple metal, Mg(0001), first-principles DFT calculation also shows the lack of a barrier on the adiabatic PES,[23] which is in strong disagreement with experimental observation[24,25] of a low sticking coefficient of O_2 at Mg(0001). This discrepancy was ascribed, in a similar manner with that in the O_2/Al(111) system, to nonadiabaticity in the dissociation process of oxygen molecules.[23]

Therefore, it becomes clear that the theoretical study of oxygen dissociation at the simple *sp* metals is still far from its maturity. In particular, considering the fact that up to now most of the theoretical results and conclusions are only based on the O_2/Al(111) and O_2/Mg(0001) prototypes, workers are thus confronted with an important question. Does it remain necessary or valid for all simple *sp* metals (at least, for metals with similar elemental valence electrons to Al or Mg) that take into account such nonadiabaticity as spin-selection rule in obtaining an activated PES? Motivated by this question, in this paper we have carried out a systematic *ab initio* investigation of the adsorption and dissociation of oxygen molecules at Be(0001) surface. Beryllium has the same crystal structure and valence electrons as magnesium does. Subsequently, it is attempting for one to derive that the behaviors of oxygen dissociation at Be(0001) are the same as or similar to those at Mg(0001). Our results, however, show that this is not true. The most distinct is that in the present O_2/Be(0001) system, our calculated adiabatic PES displays sizeable energy barriers along the dissociation paths. This partially but definitely answers the above question. That is, in the DFT calculations of the simple-metal systems, the inclusion of nonadiabatic effects is not always indispensable for the presence of molecular dissociation barrier.

Besides this basic point of interest, our present study is also motivated by the fact that Be has vast technological applications due to its high melting point and low weight. During these applications, surface oxidation as the main kind of corrosion always needs to be prevented. Thus a systematic study on the adsorption and dissociation of O_2 molecules at Be surfaces, i.e., the initial stage during surface oxidation process, should be done. Moreover, Be is also a getter in experimental nuclear fusion reactors to adsorb residual gases such as O_2 and H_2O in the plasma vessel, improving the plasma cleanliness,[26] which also makes it highly meaningful to study the adsorption and dissociation of O_2 at Be surfaces. At present there are only very few experimental data on oxidation of Be, reporting that the surface oxidation begins at an oxidation nucleation center, followed by a spreading growth from the center,[26–29] while *ab initio* studies are entirely lacking. This as a whole encourages us to theoretically report a systematic investigation on the O_2/Be(0001) system. The rest of this paper is organized as follows. In Sec. II the computational method is briefly described. In Secs. III and IV we present our results for O_2 adsorption and dissociation at Be(0001) surface, respectively. Finally, we close our paper with a summary of our main results.

II. COMPUTATIONAL METHOD

The DFT total-energy calculations were carried out using the Vienna *ab initio* simulation package[30] with the projector-augmented-wave (PAW) pseudopotentials[31] and plane waves. The clean $p(2\times2)$-Be(0001) surface was modeled by periodic slabs consisting of nine Be layers separated by a vacuum of 20 Å, which was found to be sufficiently convergent. Oxygen molecules were symmetrically introduced on both sides of the slab. During our calculations, the positions of the outmost three Be layers as well as the O_2 molecules were allowed to relax until the forces on the ions were less than 0.02 eV/Å, while the central three layers of the slab were fixed in their calculated bulk positions. The plane-wave energy cutoff was set to 400 eV. After a careful convergence analysis, we used a $11\times11\times1$ k-point grid for the $p(2\times2)$ cell with the Monkhorst-Pack scheme.[32] Furthermore, the generalized gradient approximation (GGA) of Perdew *et al.*[33] for the exchange-correlation potential was employed since the GGA results has been previously validated for bulk Be.[34] A Fermi broadening[35] of 0.1 eV was chosen to smear occupation of the bands around E_F by a finite-T Fermi function and extrapolating to $T=0$ K.

First, the total energy of the bulk hcp Be was calculated to obtain lattice parameters. The calculated lattice constants are 2.26 and 3.56 Å, respectively, for a and c, according to the experimental values[36] of 2.285 and 3.585 Å. The calculation of the clean $p(2\times2)$-Be(0001) surface shows that the two outmost Be(0001) layers relax significantly from the bulk values. The first-second interlayer expansion is 3.8% and the second-third interlayer contraction is nearly 1.2%, which is in agreement with recent first-principles calculations[37] and comparable with experimental measurements.[38] The total energies of the isolated O atom and free O_2 molecule are calculated in an orthorhombic cell of scale $13\times11\times17$ Å^3 with a $(3\times3\times3)$ k-point mesh for the Brillouin-zone sampling. The spin-polarization correction was included. The binding energy of O_2 is calculated to be $1/2E_b^{O_2}=2.89$ eV per atom and the O-O bond length is about 1.235 Å. These results are typical for well-converged DFT-GGA calculations. Compared to the experimental[39] values of 2.56 eV and 1.21 Å for O binding energy and bonding length, the usual DFT-GGA result always introduces an overestimation, which reflects the theoretical deficiency for describing the local orbitals of the oxygen.

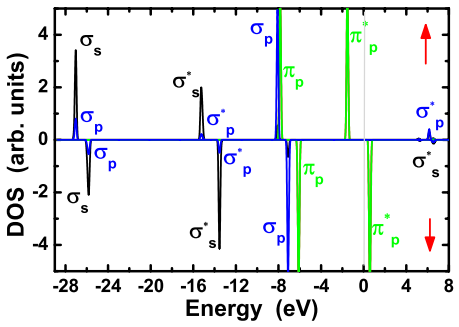

FIG. 1. (Color online) The calculated spin-polarized density of states for the MOs of the free O_2 molecule. The Fermi energy level is set at zero.

Moreover, in order to show the general charge-transfer or redistribution effects on O_2 molecular orbits (MOs) after adsorption, here we first calculate and plot in Fig. 1 the MO-resolved local density of states of the free O_2 molecule. Typically, the bonding σ MOs are lower in energy than the bonding π MOs for both spins. This ordering of the MOs has important consequences for the molecular bond to the surface. Also it reveals in Fig. 1 that spin splittings are sizeable ($\sim$2 eV) for both bonding and antibonding MOs. This reflects Hund's spin rule, which describes ground state as spin polarized for O_2 ($S=1$). The highest occupied MO (HOMO) and the lowest unoccupied MO (LUMO) are the spin-up and spin-down antibonding π^* MOs, respectively. Our calculated picture of the MOs for a free O_2 molecule is in good agreement with previous theoretical reports.[20,40]

III. ADSORPTION OF O_2 MOLECULE

There are four high-symmetry adsorption sites on the Be(0001) surface, including top (T), hcp hollow (HH), fcc hollow (FH), and bridge (B) sites depicted in Fig. 2(a). In this study, we construct twelve initial structures with high symmetries by orienting the O_2 molecule at the four high-symmetry sites, respectively, along the X (i.e., $[11\bar{2}0]$), Y (i.e., $[\bar{1}100]$), and Z (i.e., [0001]) directions. We also construct several low-symmetry initial structures by rotating the O_2 molecule in the XY, YZ, and XZ planes with small angles. In all the initial configurations, the heights of the O_2 molecules are set at $h_0=4$ Å, see Fig. 2(b). It is found within our expectation that after geometry optimization, these low-symmetry structures will either relax into the high-symmetry ones or be less stable with a lower adsorption energy than the high-symmetry ones. This is similar to what has been ob-

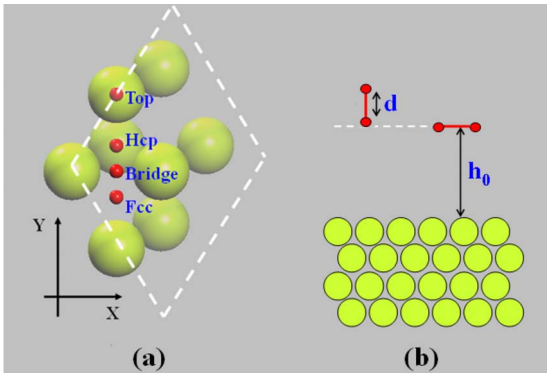

FIG. 2. (Color online) (a) The $p(2\times2)$ surface cell of Be(0001) and four on-surface adsorption sites. Here only the outmost two layers of the surface are shown. (b) The sketch map shows that the molecule (with vertical or parallel orientation) is initially away from the surface with a high h_0. Note that although the atomic radius of O is much larger than that of Be, for convenience in depicting the adsorption positions, here and in the following we use larger circles to denote Be atoms.

served in studying the adsorption of O_2 molecules at Pb(111).[41] After geometry optimization, it is found that all the parallel adsorption states with the O_2 molecule lying down on the substrate surface are stable. For the vertical entrances with the O_2 molecule oriented perpendicular to the surface, one exception is the B-*Z* entrance (namely, the O_2 molecule at the bridge site with the O-O bond along the *Z* direction), which turns to evolve into the HH-*Z* adsorption configuration after geometry optimization.

One central quantity tailored for the present study is the average adsorption energy of the adsorbed oxygen species defined as

$$E_{\mathrm{ad}} = -\frac{1}{N_{\mathrm{O}}}\left[E_{\mathrm{O_2/Be(0001)}} - E_{\mathrm{Be(0001)}} - N_{\mathrm{O}}\frac{1}{2}E_{\mathrm{O_2}}\right], \qquad (1)$$

where N_{O} is the total number of O atoms presented in the supercell, $E_{\mathrm{O_2/Be(0001)}}$, $E_{\mathrm{Be(0001)}}$, and $E_{\mathrm{O_2}}$ are the total energies of the slab containing oxygen, of the corresponding clean Be(0001) slab, and of a free O_2 molecule, respectively. According to this definition, a positive value of E_{ad} indicates that the adsorption is exothermic (stable) with respect to a free O_2 molecule and a negative value indicates endothermic (unstable) reaction.

Starting from the abovementioned entrances and after geometry optimization, the obtained molecular adsorption energy (E_{ad}), molecular magnetic moment (MM), work function (Φ), adsorption height (h), and O-O bond length (d) are listed in Table I. From Table I one can clearly see the prominently different molecular adsorption features along the parallel and vertical channels. (i) For the O_2 molecule in parallel with Be(0001) surface, the relaxed molecular structures vary very little compared to the initial molecular structures, which suggests the molecular adsorption to be the physisorption in these parallel channels. In these cases, the relaxed adsorption height is around 3.9 Å. The O-O bond length is 1.236 Å, displaying a negligible expansion when compared to that of a free O_2 molecule (1.235 Å). The molecular MM almost saturates at its free value of $2.0\mu_B$, also suggesting the almost unaffected molecular orbitals in these physisorbed structures. In addition, the work function of the adsorbed Be(0001) surface is almost identical to that of the clean Be(0001) surface, implying negligible charge transfer between the parallel O_2 adsorbate and the surface Be atoms. Finally, the calculated molecular adsorption energy is only ~23 meV, which is so small that a little thermal fluctuation may result in desorption of the O_2 adsorbate with parallel O-O bond from the Be(0001) surface. This result is consistent with recent experimental observation that the reactivity of oxygen atoms with Be(0001) surface is greater than that of oxygen molecules with Be(0001) surface.[29] On the other hand, one may question whether, when overcoming the energy barrier by artificially setting the initial metal-molecule distance h_0 to be lower than the above-obtained physisorption height (~3.9 Å), different kinds of molecular adsorption state with parallel O-O bond will occur or not. For this, a large amount of calculations with lower initial adsorption heights have been carried out and no other parallel molecular physisorption or chemisorption states have been found, for details see discussion in Sec. IV. (ii) For the O_2 adsorbate with the O-O bond oriented perpendicular to Be(0001) surface, as shown in Table I, the relaxed molecular structures display a signature of chemisorption. Among them the HH-*Z* configuration is most stable with the largest molecular adsorption energy of ~0.5 eV (per atom). In this channel the adsorption height is decreased to be 1.58 Å, and prominently, the molecular MM is largely decreased to be $0.8\mu_B$, which suggests a pronounced charge redistribution among the MOs via interaction with the Be(0001) surface. The O-O bond in this most stable chemisorption channel is 1.471 Å, indicating a large expansion from the free O_2 molecule and a fundamental weakening of the molecular bonding. In addition, the work-function change is also prominent, implying an observable charge redistribution between the chemisorbed O_2 molecule and the Be(0001) surface. Meanwhile, during

TABLE I. The calculated adsorption energy per atom (E_{ad}), molecular MM, work function (Φ), adsorption height (h), and O-O bond length (d) for physisorptions and chemisorptions along different channels.

	Channel	E_{ad} (meV)	MM (μ_B)	h (Å)	d (Å)	Φ (eV)
	T-*X*	23.6	1.97	3.92	1.236	5.44
	T-*Y*	23.1	1.95	3.91	1.236	5.44
	B-*X*	23.9	1.97	3.91	1.236	5.44
Physisorption	B-*Y*	22.5	1.97	3.93	1.236	5.46
	HH-*X*	23.8	1.99	3.91	1.236	5.45
	HH-*Y*	23.3	2.0	3.9	1.236	5.43
	FH-*X*	23.7	1.99	3.92	1.236	5.46
	FH-*Y*	22.6	1.99	3.92	1.236	5.46
	T-*Z*	75.2	1.5	2.1	1.272	6.76
Chemisorption	HH-*Z*	506.1	0.8	1.15	1.471	7.78
	FH-*Z*	377.6	0.9	1.28	1.436	7.63

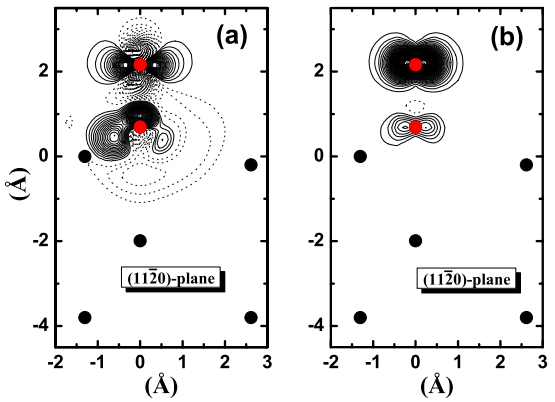

FIG. 3. (Color online) Contour plots of (a) the difference electron density and (b) the spin density for the relaxed O_2/Be(0001) slab with O_2 molecule chemisorbed along the HH-*Z* entrance. Solid and dotted lines denote accumulated and depleted densities, respectively.

chemisorption of the O_2 molecule, the Be(0001) surface is also influenced. Specifically, the three Be atoms around the adsorbed O_2 molecule of the HH-*Z* entrance are pulled out by about 0.3 Å. Recalling that the bulk BeO has an unusual wurtzite structure, it is within one's expectation that O_2 chemisorption in the HH-*Z* channel (instead of the FH-*Z* channel) is most energetically favorable. Our additional calculations of the atomic oxygen adsorption at Be(0001) also show that the hcp hollow site is most stable for atomic oxygen adsorption.

To clarify the bonding interaction between the chemisorbed O_2 molecule (in the HH-*Z* channel) and the Be(0001) surface, we calculate and plot in Fig. 3(a) the electron-density difference $\Delta\rho(\mathbf{r})$, which is obtained by subtracting the electron densities of noninteracting component systems, $\rho_{\mathrm{Be(0001)}}(\mathbf{r})+\rho_{\mathrm{O_2}}(\mathbf{r})$, from the density $\rho_{\mathrm{O_2/Be(0001)}}(\mathbf{r})$ of the O_2/Be(0001) system, while retaining the atomic positions of the component systems at the same location as in O_2/Be(0001). A positive $\Delta\rho(\mathbf{r})$ obviously represents charge accumulation, whereas a negative $\Delta\rho(\mathbf{r})$ represents charge depletion. One can see from Fig. 3(a) (where the contour spacing is $0.02e/\text{Å}^3$) that the charge redistribution mainly occurs at the surface and involves the chemisorbed O_2 molecule and the two topmost Be (0001) layers. It is apparent that upon molecular chemisorption, the occupation of the surface and subsurface Be *sp* states is decreased, while the occupation of O_2 π^* antibonding MOs is increased, which suggests an electron transfer from the former to the latter. Meanwhile, it reveals in Fig. 3(a) that the occupation of other bonding (σ,π) and antibonding MOs (σ^*) is also decreased. The target states for these transferred MO charges are of course again the O_2 π^* antibonding MOs, as shown in Fig. 3(a). A well-known harpooning mechanism is responsible for this inter-MO charge transfer. Prominently, the electron redistribution of the O_2 π^* antibonding MOs is largely asymmetric with respect to the two O atoms. The reason is that the lower O atom in the O_2 molecule is in a complex bonding state. Besides interacting with the upper O atom to form a weakly bound molecule, this lower O atom also strongly interacts with surface and subsurface Be atoms via a

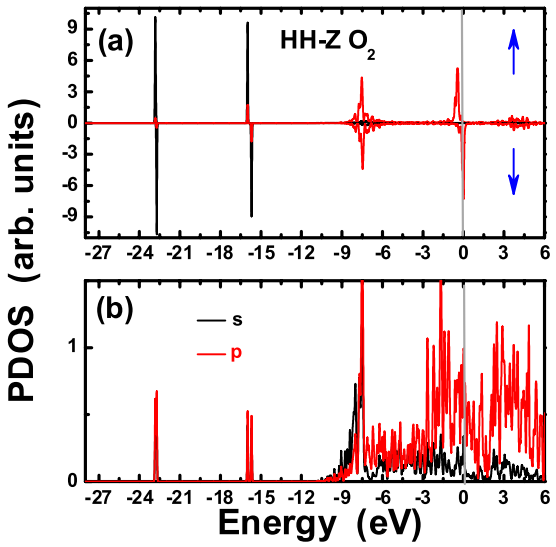

FIG. 4. (Color online) The orbital-resolved PDOS for the chemisorbed O_2 molecule along the HH-*Z* channel and (b) for the topmost Be layer. The Fermi energy is set at zero. Note that for O_2 the PDOS is plotted in a spin-split form.

mixed ionic/covalent bonding mechanism. In particular, it is the strong covalency in the Be-O bond that heavily distorts the charge distribution of the O_2 π^* antibonding MOs. To our knowledge, this strong covalency in the bond between the metal surface and the O_2 molecule has not been theoretically reported in previous studies. On the whole, the charge transfer to the π^* antibonding MOs, as well as the strong covalency in the Be-O bond, weakens the molecular bond and spin polarization. For spin density of the chemisorbed O_2 molecule in the HH-*Z* channel, see Fig. 3(b).

In order to gain more insights into the precise nature of the chemisorbed molecular state in the O_2/Be(0001) system, the orbital-resolved site-projected densities of states (PDOS) for the O_2 molecule (in the most stable HH-*Z* entrance) and the topmost Be layer are plotted in Figs. 4(a) and 4(b), respectively. By comparison with the case of a free O_2 molecule, one can see that the MO properties of the chemisorbed O_2 in the HH-*Z* entrance undergo the following fundamental changes. (i) The spin-split PDOS signature (peaks) for the two energy-lowest bonding and antibonding σ MOs for both spins in Fig. 1 changes prominently, indicating their strong perturbation by interacting with the Be(0001) surface. This is in accord with the electron-density difference result shown in Fig. 3(a) that charges mostly flow out of these two MOs. (ii) The PDOS peaks for the two nearly degenerate bonding σ_p and π_p MOs around $E=-7.5$ eV are broadened upon chemisorption to merge together, with the amplitude becoming much weaker than that in free O_2. Also, the spin splitting of these two bonding MOs vanishes. These features consistently reveal that although these two bonding MOs do not lose their nature as the MOs, they are largely reshaped due to their hybridization with the *sp* orbitals of the surface and subsurface Be atoms. This metal-molecule hybridization is so strong that there develops, as shown in Fig. 4, a sharp *sp*-hybrid peak around $E=-7.5$ eV in the PDOS for the topmost Be layer. (iii) The spin-up antibonding π_p^* MO shifts up

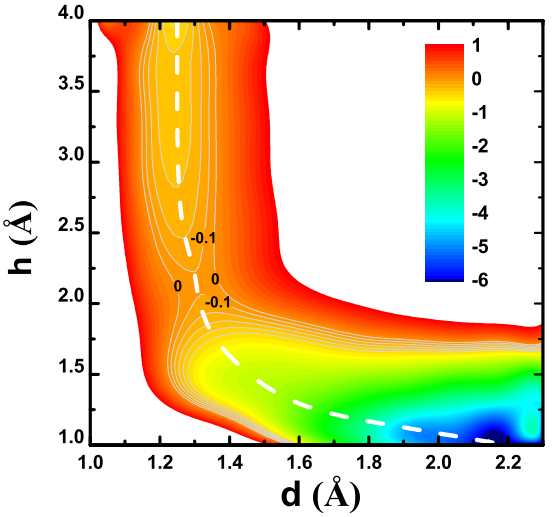

FIG. 5. (Color online) Color-filled contour plot of the potential energy surface for O_2 dissociation at Be(0001) along the T-Y channel, as functions of the O_2 bond length d and distance h (from the surface). The contour spacing is 0.1 eV. The dashed line indicates the reaction pathway.

in energy toward E_F and is partially depopulated by an observable amount of charges. As a compensation, the spin-down antibonding π_p^* MO shifts down toward E_F and becomes partially occupied. Obviously, the spin rule prohibits direct charge transfer from spin-up to spin-down antibonding π_p^* MO. Therefore, the driving or intermediate factor for this charge decrease in the spin-up and increase in the spin-down π_p^* MOs is due to the metallic Be(0001) surface, which accepts electrons from the spin-up π_p^* MO and then donates electrons to the spin-down π_p^* MO. From this aspect, the present result is consistent with the well-known harpooning mechanism, which describes adsorbate-metal interaction by a simultaneous transfer of electrons from the adsorbing molecule into the unoccupied metal states (direct bonding) and a back donation of electrons from occupied metal states into the antibonding adsorbate orbitals. In the present case, this exchange is achieved through interaction with the *sp* orbitals of the Be(0001) surface. (iv) There develops a different hybrid peak at $E=-22.7$ eV in the PDOS of the system. From Fig. 4 one can see that this peak is characterized by a strong hybridization of O 2*s* and Be *sp* states.

IV. DISSOCIATION OF O_2 MOLECULES

In order to deepen our understanding of the initial stage of oxidation at Be(0001) surface from a theoretical point of view, we also calculate the potential energy surfaces (PESs) for O_2 molecules on the Be(0001) surface, which depicts the adiabatic dissociation path with the lowest-energy barrier. Since it has been shown that the PES given by the density-functional theory gives the result that can be compared with experiments, we expect that our calculated PES provides the qualitative feature of the molecular dissociation process in the present specific O_2/Be(0001) system. Figure 5 shows the obtained PES as a function of the distance h from the surface and the bond length d of the O_2 molecule along the T-Y channel, which, after a large amount of calculations, turns out to be the most favorable dissociative adsorption channel with largest adsorption energy (4.14 eV/atom) and lowest activation barrier (0.23 eV).

One can clearly see from Fig. 5 the energetic process from initial molecular physisorption with a height of 3.9 Å and bond length of 1.23 Å to final dissociative adsorption. The most distinct feature in Fig. 5 is that the calculated adiabatic PES exhibits a sizeable energy barrier toward dissociative adsorption. The transition state for this barrier is located at a distance of 2.2 Å from the Be surface, where the O-O bond length is elongated to 1.30 Å. Correspondingly, if we initially put O_2 in the T-Y channel at a height lower than 2.2 Å, then perform geometry optimization, the O_2 molecule will spontaneously dissociate with the two O atoms moving to the hcp and fcc hollow sites, respectively. Considering that the previous *ab initio* calculations have failed to obtain a barrier on the adiabatic PES for oxygen dissociation on the usual simple metals such as Al(111) and Mg(0001), obviously, our present prediction of the activated PES in the O_2/Be(0001) system is unique. In particular, since beryllium has the same crystal structure and valence electrons as magnesium does, it is attempting to assume that the behavior of oxygen dissociation at Be(0001) is the same as or similar to that at Mg(0001). The result in Fig. 5, however, shows that this intuitive expectation needs to be reshaped.

In the case of Al(111) or Mg(0001), the failure of adiabatic DFT calculations in producing an activated-type PES has been ascribed to the unphysical output that charge transfer occurs even at large molecule-metal distance, which has led to speculations that nonadiabatic effects may play an important role in the oxygen dissociation process at these metal surfaces with simple *sp* bands.[13,15–21,23] The unphysical charge transfer at large molecule-metal distance is generally caused by the requirement in the adiabatic description that the electron chemical potential of the O_2 molecule aligns with that of the metal surface in the combined system (metal plus molecule). On the other hand, however, this requirement does not necessarily result in artificial charge transfer between the two largely separated subsystems. To date there is no universal criterion available to judge whether the adiabaticity during molecular dissociation process breaks down or not. The molecule-metal interaction is so species sensitive that even for the two metals with the same crystal structure and valence electrons, the molecular dissociation process at the surfaces can display qualitatively different behaviors. To make more sense, we have carried out a comparative study on the long-distance charge-transfer effect by choosing the metal surfaces as Be(0001), Mg(0001), and Al(111). The distances of the O_2 molecule from the three kinds of metal surfaces are fixed at the same value of 7 Å, at which charge transfer should not occur in reality. Also, the O_2 molecules in the three systems are identically chosen to be in the HH-Z entrance. The calculated spin-split PDOS for the O_2 molecule and the charge-density difference $\Delta\rho(\mathbf{r})$ in the three systems are shown in Fig. 6. Clearly, one can see that for O_2/Al(111) and O_2/Mg(0001), although the distance of the O_2 molecule from the surfaces is set to be as large as 7 Å and charge transfer should not occur in real systems, the

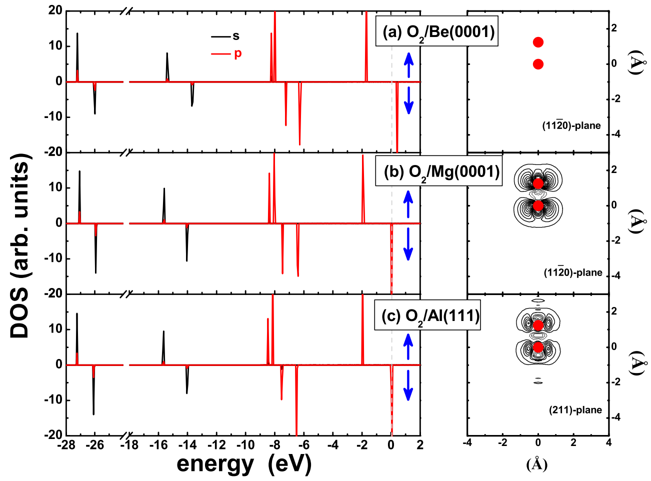

FIG. 6. (Color online) Spin-polarized DOS for the molecular orbits of O_2 with a fixed vertical distance of 7 Å from (a) Be(0001), (b) Mg(0001), and (c) Al(111) surfaces. The O-O bond length in each case is allowed to relax. The corresponding charge-density differences $\Delta\rho(\mathbf{r})$ are plotted on the right side with the contour spacing of $0.002/\text{Å}^3$. Solid and dotted lines denote the accumulated and depleted densities, respectively.

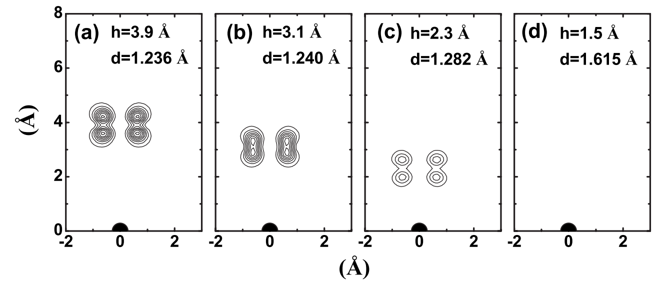

FIG. 7. Snapshots of the spin quenching process during O_2 dissociation at Be(0001) along the T-Y channel. The spacing of the spin-density contours is $0.2\mu_B/\text{Å}^3$. The corresponding O_2 molecular bond length d and distance h from the surface are also indicated.

adiabatic DFT calculations give yet the contrary results. In these two cases, it reveals in Figs. 6(b) and 6(c) that the LUMO of the ideal O_2 molecule (i.e., the spin-down antibonding π_p^* MO) has shifted down to align with the Fermi energy and becomes partially occupied, accompanying an observable decreasing of the molecular spin. The O-O bond length also undergoes a little expansion compared to the free value of 1.235 Å. Actually, it is exactly due to this unphysical (metal-molecule or intramolecule) charge transfer depicted in Figs. 6(b) and 6(c) that motivates theoretical workers to remedy the calculations by, for example, nonadiabatically constraining the molecular spins. As a direct result, a sizeable energy barrier will appear on the corrected PES.[21] When the attention is paid to the O_2/Be(0001) system, however, we find that such unphysical large-distance charge-transfer effect does not happen in the calculation. In fact, from Fig. 6(a) one can see that at a metal-molecule distance of 7 Å, the calculated spin-split molecular PDOS shows no change with respect to the free case. The LUMO remains empty and the charge-density difference is zero everywhere. Subsequently, the molecular bond length and spin of O_2 are not influenced at all by the presence of the Be(0001) surface at a distance of 7 Å. Combining with Fig. 5, therefore, we conclude that unlike Al(111) and Mg(0001), the adiabatic DFT calculation presented in this paper is suf-

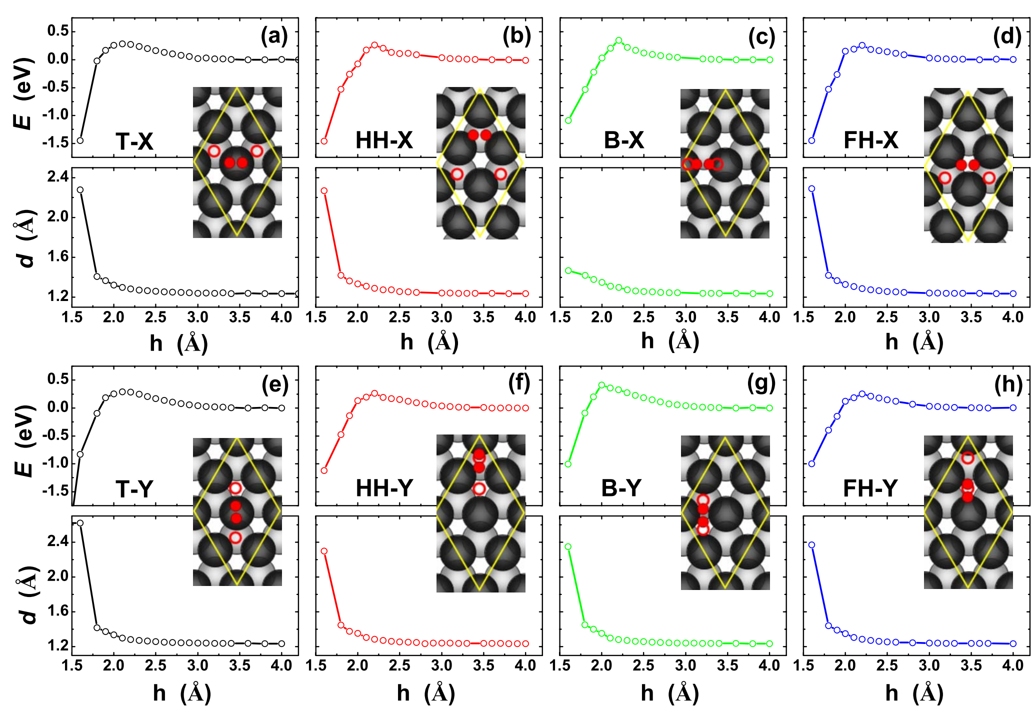

FIG. 8. (Color online) One-dimensional cuts of the potential energy surfaces and the corresponding O-O bond lengths as functions of the O_2 distance h from the surface for eight different dissociative channels. The inset in each panel indicates the initial (filled circles) and final (hollow circles) atomic positions of O_2.

TABLE II. The calculated dissociative adsorption energy (E_{ad}), dissociative energy barrier (ΔE), and geometric parameters (namely, the O_2 molecular bond length d_{TS} and distance h_{TS} from the surface) of the transition state along the eight different dissociation channels.

Channel	E_{ad} (eV)	ΔE (eV)	h_{TS} (Å)	d_{TS} (Å)
T-*X*	4.00	0.28	2.10	1.30
T-*Y*	4.14	0.23	2.10	1.30
B-*X*	3.99	0.26	2.20	1.29
B-*Y*	4.10	0.26	2.20	1.29
HH-*X*	3.81	0.35	2.20	1.30
HH-*Y*	4.09	0.41	2.10	1.30
FH-*X*	4.00	0.25	2.20	1.29
FH-*Y*	4.10	0.25	2.20	1.28

ficient to predict an activated-type dissociation process of O_2 at Be(0001).

For further illustration of O_2 dissociation at Be(0001), we plot in Fig. 7 four snapshots for the spin density (the contour spacing is $0.2\mu_B/Å^3$) evolving along the dissociation path shown in Fig. 5. The values of the corresponding heights h and relaxed bond lengths d of the O_2 molecule are also indicated in the figure. One can see from Fig. 7 that as the O_2 molecule approaches the surface along the T-*Y* channel, the O-O bond length increases, while the spin magnetic moment decreases and tends to vanish at $h \sim 2.3$ Å. Since there has occurred electron transfer from the substrate to the molecule at this height, thus the disappearance of the spin moment is due to the donation of the minority spins from the substrate and not due to the spin flip inside the molecule.

The adiabatic PESs for O_2 dissociation at Be(0001) along the other parallel channels have also been calculated, which are found to have very similar elbow shapes except for visible differences in the transition states and dissociation barriers. To be clearer, a detailed comparison of these PESs is depicted in Fig. 8 by separately plotting the one-dimensional cuts of PESs and O-O bond length as functions of the O_2 height h from the substrate surface. The inset in each panel in Fig. 8 displays the initial and final positions of the two O atoms. Clearly, the dissociative adsorption of O_2 along each of these parallel channels is a direct and activated type. The obtained dissociative adsorption energies, the dissociative energy barriers, and the geometrical parameters for the corresponding transition states, including the height of the O_2 molecule and the O-O bond length, are concluded in Table II. It is found that the dissociation path with both the lowest-energy barrier and the largest dissociative adsorption energy is along the T-*Y* channel. For all the dissociation paths, the O-O bond lengths at the transition states are similar, ranging from 1.28 to 1.30 Å. Note that no dissociative adsorptions are found for the O_2 molecules along the vertical entrances, which thus are not plotted in Fig. 7 and listed in Table II. This is different from the O_2/Al(111) system, in which molecular dissociation along vertical channels has been predicted to occur as well.[12]

V. CONCLUSION

In summary, by performing *ab initio* simulations we have systematically investigated the adsorption and dissociation of oxygen molecules on the Be(0001) surface. We have identified physisorbed and chemisorbed molecular states, which directly occur along the parallel and vertical channels, respectively. For the most stable chemisorbed molecular state (which is along the HH-*Z* entrance), in particular, we have studied its electronic and magnetic properties by calculating the charge-density difference, the spin density, and the PDOS, which clearly show the charge transfer from the spin-up π^* MO to the substrate followed by the back donation from the substrate to the spin-down π^* MO, as well as the distinct covalent weight in the chemical bonding between O_2 and Be(0001). This important covalency in the molecule-metal bond has been revealed through the following facts. (i) The charge is largely accumulated along the Be-O bond [Fig. 5(a)]. (ii) The σ, σ^*, and π MOs are heavily hybridized with the Be *sp* states (Fig. 6). (iii) The chemisorbed molecular state in the HH-*Z* channel is much stable than that in the FH-*Z* channel, implying an observable role played by the subsurface Be atom beneath the O_2 molecule.

The energy path for the dissociation of O_2 on Be(0001) surface has been determined by calculating the adiabatic PESs along various channels, among which the T-*Y* channel has been found to be the most stable and favorable one for the dissociative adsorption of O_2. Remarkably, our results have shown that the adiabatic dissociation process in the present O_2/Be(0001) system is an activated type, with the lowest-energy barrier of 0.23 eV in the most stable T-*Y* channel. We theoretically predicted a sizeable adiabatic energy barrier during dissociation of O_2 at the metal surfaces with simple *sp* bands. Thus as a final concluding remark, here we point out that in spite of many previous revealing and specific studies, an in-depth and primary insight into the common nature of the O_2 dissociation at various simple *sp* metal surfaces remains yet to be attainable.

ACKNOWLEDGMENTS

This work was supported by the NSFC under Grants No. 10604010 and No. 60776063, and by the National Basic Research Program of China (973 Program) under Grant No. 2009CB929103.

[1] G. Darling and S. Holloway, Rep. Prog. Phys. **58**, 1595 (1995).
[2] *The Chemical Physics of Solid Surfaces and Heterogeneous Catalysis*, edited by D. A. King and D. P. Woodruff (Elsevier, Amsterdam, 1988).
[3] H. H. Kung, *Transition Metal Oxides, Surface Chemistry and Catalysis* (Elsevier, Amsterdam, 1989); V. E. Henrich and P. A. Cox, *The Surface Science of Metal Oxides* (Cambridge University Press, Cambridge, England, 1994).
[4] P. Błoński, A. Kiejna, and J. Hafner, Phys. Rev. B **77**, 155424 (2008).
[5] S. Yotsuhashi, Y. Yamada, T. Kishi, W. A. Diño, H. Nakanishi, and H. Kasai, Phys. Rev. B **77**, 115413 (2008).
[6] H. Nakatsuji and H. Nakai, J. Chem. Phys. **98**, 2423 (1993).
[7] P. A. Gravil, D. M. Bird, and J. A. White, Phys. Rev. Lett. **77**, 3933 (1996).
[8] A. Eichler and J. Hafner, Phys. Rev. Lett. **79**, 4481 (1997).
[9] A. Eichler, F. Mittendorfer, and J. Hafner, Phys. Rev. B **62**, 4744 (2000).
[10] H. Brune, J. Wintterlin, J. Trost, G. Ertl, J. Wiechers, and R. J. Behm, J. Chem. Phys. **99**, 2128 (1993).
[11] L. Österlund, I. Zorić, and B. Kasemo, Phys. Rev. B **55**, 15452 (1997).
[12] T. Sasaki and T. Ohno, Phys. Rev. B **60**, 7824 (1999); K. Honkala and K. Laasonen, Phys. Rev. Lett. **84**, 705 (2000).
[13] Y. Yourdshahyan, B. Razaznejad, and B. I. Lundqvist, Solid State Commun. **117**, 531 (2001).
[14] Y. Yourdshahyan, B. Razaznejad, and B. I. Lundqvist, Phys. Rev. B **65**, 075416 (2002).
[15] B. Kasemo, Phys. Rev. Lett. **32**, 1114 (1974).
[16] B. Kasemo, R. Toernqvist, J. K. Nørskov, and B. I. Lundqvist, Surf. Sci. **89**, 554 (1979).
[17] G. Katz, Y. Zeiri, and R. Kosloff, J. Chem. Phys. **120**, 3931 (2004).
[18] A. M. Wodtke, J. C. Tully, and D. J. Auerbach, Int. Rev. Phys. Chem. **23**, 513 (2004).
[19] A. Hellman, B. Razaznejad, Y. Yourdshahyan, H. Ternow, I. Zorić, and B. I. Lundqvist, Surf. Sci. **532-535**, 126 (2003).
[20] A. Hellman, B. Razaznejad, and B. I. Lundqvist, Phys. Rev. B **71**, 205424 (2005).
[21] J. Behler, B. Delley, S. Lorenz, K. Reuter, and M. Scheffler, Phys. Rev. Lett. **94**, 036104 (2005); J. Behler, K. Reuter, and M. Scheffler, Phys. Rev. B **77**, 115421 (2008).
[22] X. L. Fan, W. M. Lau, and Z. F. Liu, Phys. Rev. Lett. **96**, 079801 (2006).
[23] A. Hellman, Phys. Rev. B **72**, 201403(R) (2005).
[24] S. M. Driver, J. Lüdecke, G. J. Jackson, and D. P. Woodruff, J. Electron Spectrosc. Relat. Phenom. **98-99**, 235 (1999).
[25] L. Aballe, A. Barinov, A. Locatelli, S. Heun, and M. Kiskinova, Phys. Rev. Lett. **93**, 196103 (2004).
[26] S. Zalkind, M. Polak, and N. Shamir, Surf. Sci. **385**, 318 (1997).
[27] S. Zalkind, M. Polak, and N. Shamir, Surf. Sci. **513**, 501 (2002).
[28] S. Zalkind, M. Polak, and N. Shamir, Phys. Rev. B **71**, 125413 (2005).
[29] Ch. Linsmeier and J. Wanner, Surf. Sci. **454-456**, 305 (2000).
[30] G. Kresse and J. Hafner, Phys. Rev. B **47**, 558 (1993); G. Kresse and J. Furthmüller, Comput. Mater. Sci. **6**, 15 (1996); G. Kresse and J. Furthmüller, Phys. Rev. B **54**, 11169 (1996).
[31] G. Kresse and D. Joubert, Phys. Rev. B **59**, 1758 (1999).
[32] H. J. Monkhorst and J. D. Pack, Phys. Rev. B **13**, 5188 (1976).
[33] J. P. Perdew, J. A. Chevary, S. H. Vosko, K. A. Jackson, M. R. Pederson, D. J. Singh, and C. Fiolhais, Phys. Rev. B **46**, 6671 (1992).
[34] E. Wachowicz and A. Kiejna, J. Phys.: Condens. Matter **13**, 10767 (2001).
[35] M. Weinert and J. W. Davenport, Phys. Rev. B **45**, 13709 (1992).
[36] V. M. Amonenko, V. Ye. Ivanov, G. F. Tikhinskij, and V. A. Finkel, Phys. Met. Metallogr. **14**, 47 (1962).
[37] M. Lazzeri and S. de Gironcoli, Phys. Rev. Lett. **81**, 2096 (1998).
[38] K. Pohl, J.-H. Cho, K. Terakura, M. Scheffler, and E. W. Plummer, Phys. Rev. Lett. **80**, 2853 (1998); H. L. Davis, J. B. Hannon, K. B. Ray, and E. W. Plummer, *ibid.* **68**, 2632 (1992).
[39] K. P. Huber and G. Herzberg, *Molecular Spectra and Molecular Structure IV: Constants of Diatomic Molecules* (Van Nostrand Reinhold, New York, 1979).
[40] A. Eichler, F. Mittendorfer, and J. Hafner, Phys. Rev. B **62**, 4744 (2000).
[41] Y. Yang, G. Zhou, J. Wu, W. H. Duan, Q. K. Xue, B. L. Gu, P. Jiang, X. C. Ma, and S. B. Zhang, J. Chem. Phys. **128**, 164705 (2008).